Estimation of Self-Exchange Electron Transfer Rate Constants for Organic Compounds from Stopped-Flow Studies

Stephen F. Nelsen,*,† Michael T. Ramm,† Rustem F. Ismagilov,† Mark A. Nagy,† Dwight A. Trieber, II,† Douglas R. Powell,† Xi Chen,‡ Jamie J. Gengler,‡ Qinling Qu,‡ Jennifer L. Brandt,‡ and Jack R. Pladziewicz*,‡

Contribution from the Department of Chemistry, University of Wisconsin, Madison, Wisconsin 53706-1396, and Department of Chemistry, University of Wisconsin, Eau Claire, Wisconsin 54702

Received January 30, 1997[⊗]

Abstract: Second-order rate constants k_{12}(obsd) measured at 25 °C in acetonitrile by stopped-flow for 47 electron transfer (ET) reactions among ten tetraalkylhydrazines, four ferrocene derivatives, and three *p*-phenylenediamine derivatives are discussed. Marcus's adiabatic cross rate formula $k_{12}(\text{calcd}) = (k_{11}\,k_{22}\,k_{12}\,f_{12})^{1/2}$, $\ln f_{12} = (\ln K_{12})^2/4\ln(k_{11}k_{22}/Z^2)$ works well to correlate these data. When all k_{12}(obsd) values are simultaneously fitted to this relationship, best-fit self-exchange rate constants, k_{ii}(fit), are obtained that allow remarkably accurate calculation of k_{12}(obsd); $k_{12}(\text{obsd})/k_{12}'(\text{calcd})$ is in the range of 0.55−1.94 for all 47 reactions. The average $\Delta\Delta G_{ij}^{\ddagger}$ between observed activation free energy and that calculated using k_{ii}(fit) is 0.13 kcal/mol. Simulations using Jortner vibronic coupling theory to calculate k_{12} using parameters which produce the wide range of k_{ii} values observed predict that Marcus's formula should be followed even when V is as low as 0.1 kcal/mol, in the weakly nonadiabatic region. Tetracyclohexylhydrazine has a higher k_{ii} than tetraisopropylhydrazine by a factor of ca. 10. Replacing the dimethylamino groups of tetramethyl-*p*-phenylenediamine by 9-azabicyclo[3.3.1]nonyl groups has little effect on k_{ii}, demonstrating that conformations which have high intermolecular aromatic ring overlap are not necessary for large ET rate constants. Replacing a γ CH_2 group of a 9-azabicyclo[3.3.1]nonyl group by a carbonyl group lowers k_{ii} by a factor of 17 for the doubly substituted hydrazine and by considerably less for the doubly substituted *p*-phenylenediamine.

Introduction

Three previous studies of intermolecular electron transfer (ET) reactions involving hydrazines using stopped-flow measurements of rate constants have been reported.[1−3] In the work discussed here a purified, isolable cation radical dissolved in acetonitrile containing 0.1 M tetrabutylammonium perchlorate is injected into a stopped-flow cell along with a neutral compound of lower formal redox potential ($E^{\circ\prime}$) in the same solvent, and the change in absorbance resulting from the ET reaction which ensues is followed as a function of time. A series of experiments varying the concentrations, carried out under pseudo-first-order conditions if possible, is used to determine the second-order rate constant, k_{12}(obsd), for the reaction. Ten of the compounds employed, shown in Scheme 1 except for **FeCp′$_2$**, have had their self-exchange rate constants, k_{ii}(self), independently measured under self-exchange conditions. They include *N*,*N*,*N*′,*N*′-tetramethyl-*p*-phenylenediamine (**TMPD**), three methylated ferrocenes, and six tetraalkylhydrazines. Table 1 summarizes the k_{ii}(self) values and formal oxidation potentials ($E^{\circ\prime}$) measured by cyclic voltammetry. The total range of k_{ii}(self) values is a factor of 5×10^{11} (15.9 kcal/mol spread in $\Delta G_{ii}^{\ddagger}$(self)) and the equilibrium constants (K_{12}), for the reactions studied range from 1 to 2×10^{13} ($\Delta G^{\circ} = 0$ to −18.2 kcal/mol). These reactions therefore provide stringent tests for the general utility of the Marcus cross rate equation (eq 1).[4]

Scheme 1

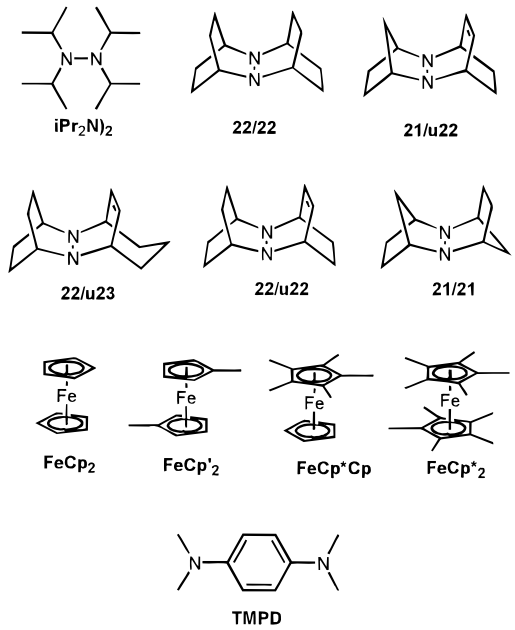

$$k_{12}(\text{calcd}) = (k_{11}k_{22}K_{12}\,f_{12})^{1/2} \qquad (1a)$$

where

$$\ln f_{12} = (\ln K_{12})^2/4\ln(k_{11}k_{22}/Z_{11}Z_{22}) \qquad (1b)$$

The f_{12} value approaches 1 as K_{12} approaches 1, and is >0.1

† University of Wisconsin—Madison.
‡ University of Wisconsin—Eau Claire.
⊗ Abstract published in *Advance ACS Abstracts*, June 1, 1997.

(1) Nelsen, S. F.; Wang, Y.; Ramm, M. T.; Accola, M. A.; Pladziewicz, J. R. *J. Phys. Chem.* **1992**, *96*, 10654.
(2) Nelsen, S. F.; Chen, L.-J; Ramm, M. T.; Voy, G. T.; Accola, M. A.; Seehafer, T.; Sabelko, J.; Pladziewicz; J. R. *J. Org. Chem.* **1996**, *61*, 1405.
(3) Nelsen, S. F.; Ismagilov, R. F.; Chen, L. J.; Brandt, J. L.; Chen, X.; Pladziewicz, J. R. *J. Am. Chem. Soc.* **1996**, *118*, 1555.

S0002-7863(97)00321-1 CCC: $14.00

Table 1. $E^{o\prime}$, Self-Exchange ET Values Measured by Homogeneous Exchange, and Those Estimated from Cross Reactions for Compounds Employed in this Work

compound	$E^{o\prime}$ (V vs SCE)	k_{ii}(self) (M^{-1} s^{-1})[a]	$\Delta G_{ii}^{\ddagger}$ (self)	rxns[b]	k_{ii}(fit) (M^{-1} s^{-1})	$\Delta G_{ii}^{\ddagger}$ (fit)	$\Delta\Delta G^{\ddagger}$ (fit − self)[c]
			Hydrazines				
21/21$^{0/+}$	+0.01[d]	$1.85(6) \times 10^4$ [S][d]	11.63	4	2.9×10^3	12.7	1.1
22/u22$^{0/+}$	−0.241[d]	$1.21(10) \times 10^4$ [S][d]	11.88	4	1.7×10^3	13.1	1.2
22/u23$^{0/+}$	−0.298[e]	$3.84(11) \times 10^3$ [S][f]	12.56	3	2.5×10^3	12.8	0.2
21/u22$^{0/+}$	+0.058[d]	$2.29(9) \times 10^3$ [S][d]	12.87	7	9.2×10^2	13.4	0.5
22/22$^{0/+}$	−0.53[g]	~700 (dec) [S][g]	13.57	2	1.1×10^2	14.4	1.1
33N)$_2$	−0.01[d]	2.2×10^3(est) [S][d,h]	12.9	8	6.9×10^2	13.6	0.7 (est)
k33NN33	+0.22[i]			8	2.4×10^2	14.2	
k33N)$_2$	+0.45[i]			7	4.0×10^1	15.3	
cHx$_2$N)$_2$	+0.26[j]			13	2.3×10^{-2}	19.7	
iPr$_2$N)$_2$ $^{0/+}$	+0.26[k]	$3.0(3) \times 10^{-3}$ [E][j,l]	20.90	14	2.4×10^{-3}	21.0	0.1
			Ferrocenes				
FeCp*$_2$ $^{0/+}$	−0.109[d]	2.9×10^7 [F][d,m]	7.27	6	1.0×10^7	7.9	0.6
FeCp*Cp$^{0/+}$	+0.124[d]	8.5×10^6 [F][d]	8.00	6	9.9×10^6	7.9	−0.1
FeCp′$_2$ $^{0/+}$	+0.281[d]			1	1.5×10^7	7.7	
FeCp$_2$ $^{0/+}$	+0.395[d]	8.1×10^6 [F][d]	8.03	1	7.1×10^6	8.1	0.1
			PD-Derivatives				
TMPD$^{0/+}$	+0.12[d]	1.47×10^9 [P][n]	4.95	4	1.2×10^8	6.4	1.5
33)$_2$PD	+0.02[i]			3	1.8×10^8	6.2	
k33)$_2$PD	+0.29[i]			3	4.0×10^7	7.1	

[a] The method used for measurement of k_{ii}(self) is abbreviated in brackets: [S] = slow exchange rate region NMR line-broadening measurements, [E] = equilibration rate measured on the laboratory time scale using ^{2}H and ^{1}H NMR to determine concentrations of deuterium-labeled and unlabeled neutral compound, [F] = fast exchange rate region NMR line-broadening measurements, [P] = fast exchange region ESR line broadening measurements. [b] Number of reactions studied having this compound as a component (Table 2). [c] $\Delta G^{\ddagger}$(fit) − $\Delta G^{\ddagger}$(self). [d] Reference 2. [e] Wang, Y. University of Wisconsin, 1993. [f] Nelsen, S. F.; Wang, Y. *J. Org. Chem.* **1994**, *59*, 1655. [g] Nelsen, S. F.; Blackstock, S. C.; Kim, Y. *J. Am. Chem. Soc.* **1987**, *109*, 677. [h] Estimated from the value measured in CH_2Cl_2. [i] Nelsen, S. F.; Kessel, C. R.; Grezzo, L. A.; Steffek, D. J. *J. Am. Chem. Soc.* **1980**, *102*, 5482. [j] Determined in this work. [k] Reference 8. [l] Reference 3. [m] Yang, E. S.; Chan, M.-S.; Wahl, A. C. *J. Phys. Chem.* **1980**, *84*, 3094 (reports a smaller rate constant than we used; see ref 1). [n] Reference 10.

Scheme 2

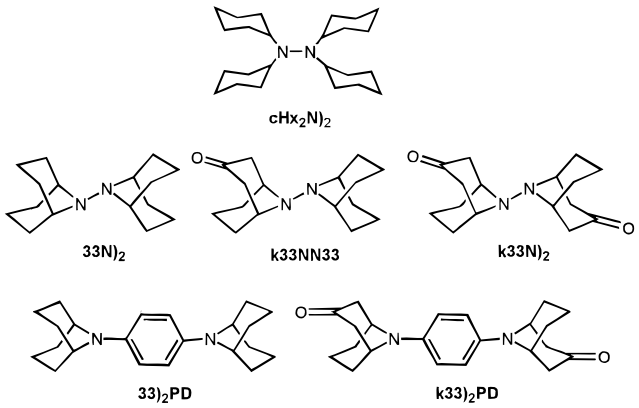

for most, but not all, of the reactions studied here. We employ preexponential factors $Z_{11} = Z_{22} = 1 \times 10^{11}$ M^{-1} s^{-1}, as has been traditional. Equation 1 is followed surprisingly well by these reactions,[1−3] encouraging us to use stopped-flow intermolecular ET studies to estimate k_{ii} values for compounds for which measurement under self-exchange conditions is not possible, and the six compounds shown in Scheme 2 are considered in this work. Their formal potentials are also shown in Table 1.

Stopped-Flow Kinetic Results and Data Treatment

Table 2 summarizes the 47 reactions considered here. Entries 1−13 are between pairs for which k_{ii}(self) for both components are known (see Table 2). For these 13 reactions it is possible to use eq 1 to calculate the cross reaction rate constant, k_{12}(calcd), and these are listed in Table 2. This approach leads to k_{12}(calcd) being higher than k_{12}(obsd). In considering the remaining 34 reactions, where one or both of the components do not have an independently measured k_{ii}(self), we were interested in extracting the most effective estimates of k_{ii} for all of the compounds, assuming the overall accuracy of eq 1. This was achieved by rearranging eq 1 in the form $\ln(k_{ii}) + \ln(k_{jj}) = A_{ij}$ and doing a least squares analysis to obtain the self-exchange rate constants k_{ii}(fit) that best fit the entire data set.[6] These k_{ii}(fit) values are given in Table 1 and used with eq 1 to calculate the expected cross reaction rate constant k_{12}'(calcd) shown for all of the reactions in Table 2. Since it is known from the 13 reactions of compounds with known k_{ii}(self) that eq 1 generally overestimates k_{12}, we did not "fix" the k_{ii} values for the "known" compounds, because this would have resulted in the entire discrepancy between k_{12}(calcd) and k_{12}(obsd) being transferred to the compounds with unknown k_{ii}(self). Equation 1 is very good at calculating k_{12} using the best fit k_{ii}(fit) values, as indicated by the ratio k_{12}(obsd)/k_{12}'(calcd) shown in the second-to-last column of Table 2. The total range of k_{12} ratios observed is 0.55−1.94, corresponding to $|\Delta\Delta G_{ij}^{\ddagger}|$ differences of ≤0.40 kcal/mol and average $|\Delta\Delta G_{ij}^{\ddagger}|$ of 0.13 kcal/mol (for comparison, the maximum and average $\Delta\Delta G_{12}^{\ddagger}$(obsd) from the errors quoted for k_{12}(obsd) are 0.12 and 0.04 kcal/mol). Twelve of the reactions studied (involving 24 components), exhibit $|\Delta\Delta G_{ij}^{\ddagger}| \geq 0.2$ kcal/mol. Of the 24 components involved in these reactions with larger deviations, six were phenylenediamine (PD)-derivatives (of the 10 PD-derivative components in reactions studied, 60% of the data set involving these components), three components were **FeCp*$_2$** (50%), eight involved the hydrazines having a twist angle about the NN bond (θ, ≈ 90°), **iPr$_2$N)$_2$** and **cHx$_2$N)$_2$** (30%), five were the $\theta \approx 180°$ **33N)$_2$**-derivatives (22%), and 2 were the $\theta \approx 0°$ hydrazines (10%). We have not discerned a way of accurately predicting which reactions will show unusually large $|\Delta\Delta G_{ij}^{\ddagger}|$ values. As noted previously with much less data,[3] varying $Z_{11}Z_{22}$ in eq 1b has only small effects on the fit of eq 1 to experimental data.[7]

(4) Marcus, R. A.; Sutin, N. *Inorg. Chem.* **1975**, *14*, 213.

(5) For reviews of ET rate theory and applications, see: (a) Marcus, R. A.; Sutin, N. *Biochim. Biophys. Acta* **1985**, *811*, 265. (b) Sutin, N. *Prog. Inorg. Chem.* **1983**, *30*, 441. (c) Sutin, N. *Acc. Chem. Res.* **1982**, *15*, 275.

(6) Pladziewicz, J. R.; Espenson, J. H. *J. Am. Chem. Soc.* **1973**, *95*, 56.

Table 2. Summary of Reactions Studied

entry	reductant	oxidant	k_{12}(obsd) (M^{-1} s^{-1})	k_{12}(calcd) (M^{-1} s^{-1})[a]	k_{12}'(calcd) (M^{-1} s^{-1})[b]	k_{12}(obsd)/ k_{12}'(calcd)	$\Delta\Delta G_{ij}^{\ddagger}$ (kcal/mol)[c]
1[d]	**22/u22**	**FeCp*$_2^+$**	$2.3(2) \times 10^6$	6.8×10^6	1.5×10^6	1.5	−0.2
2	**22/u23**	"	$5.7(3) \times 10^6$	1.0×10^7	5.0×10^6	1.1	−0.1
3[d]	**FeCp*$_2$**	**21/u22$^+$**	$1.35(23) \times 10^6$	5.5×10^6	2.1×10^6	0.6	0.3
4[e,f]	"	**iPr$_2$N)$_2^+$**	$7.6(5) \times 10^4$	2.1×10^6	1.1×10^5	0.7	0.2
5[d]	**21/u22**	**FeCp′$_2^+$**	$6.3(13) \times 10^6$	7.5×10^6	6.3×10^6	1.0	0.0
6[d]	"	**FeCp*Cp$^+$**	$3.5(5) \times 10^5$	4.9×10^6	3.3×10^5	1.0	−0.0
7[e,f]	**FeCp*Cp**	**iPr$_2$N)$_2^+$**	$1.6(1) \times 10^3$	2.1×10^3	2.0×10^3	0.8	0.1
8[e,f]	**TMPD**	"	$1.2(1) \times 10^4$	2.9×10^4	7.4×10^3	1.6	−0.3
9[e]	**21/21**	"	$2.6(2) \times 10^2$	7.6×10^2	2.7×10^2	1.0	0.0
10	**21/u22**	"	$5.5(2) \times 10^1$	1.1×10^2	6.5×10^1	0.8	0.1
11[e]	**22/22**	"	$3.2(2) \times 10^5$	6.9×10^5	2.5×10^5	1.3	−0.1
12[e]	**22/u22**	"	$1.1(1) \times 10^4$	4.0×10^4	1.3×10^4	0.8	0.1
13	**22/u23**	"	$3.1(1) \times 10^4$	5.3×10^4	3.8×10^4	0.8	0.1
14	**33)$_2$PD**	"	$4.9(6) \times 10^4$		5.2×10^4	0.9	0.0
15[e]	**33N)2**	"	$1.1(2) \times 10^2$		1.9×10^2	0.6	0.3
16	**k33NN33**	"	$1.7(2) \times 10^0$		1.6×10^0	1.0	−0.0
17	**iPr$_2$N)$_2$**	**k33N)$_2$**	$1.35(5) \times 10^1$		1.1×10^1	1.2	−0.1
18	**iPr$_2$N)$_2$**	**k33)$_2$PD$^+$**	$7.7(4) \times 10^2$		5.5×10^2	1.4	−0.2
19	**TMPD**	**cHx$_2$N)$_2^+$**	$2.1(1) \times 10^4$		2.3×10^4	0.9	0.0
20	**33)$_2$PD**	"	$8.6(3) \times 10^4$		1.6×10^5	0.5	0.3
21	**FeCp*Cp**	"	$6.2(1) \times 10^3$		6.1×10^3	1.0	0.0
22	**FeCp*2**	"	$4.0(1) \times 10^5$		3.3×10^5	1.2	−0.1
23	**21/u22**	"	$2.5(1) \times 10^2$		2.0×10^2	1.3	−0.1
24	**22/22**	"	$5.4(6) \times 10^5$		6.9×10^5	0.8	0.1
25	**22/u22**	"	$3.6(2) \times 10^4$		3.9×10^4	0.9	0.0
26	**22/u23**	"	$1.21(5) \times 10^5$		1.1×10^5	1.1	−0.0
27	**33N)$_2$**	"	$7.8(3) \times 10^2$		5.7×10^2	1.4	−0.2
28	**k33NN33**	"	$5.5(2) \times 10^0$		5.0×10^0	1.1	−0.0
29	**cHx2N)$_2$**	**k33N)$_2^+$**	$3.8(2) \times 10^1$		3.3×10^1	1.1	−0.1
30	**22/u22**	**33N)$_2^+$**	$6.3(3) \times 10^4$		7.3×10^4	0.9	0.1
31	**33N)^2**	**TMPD$^+$**	$2.0(2) \times 10^6$		3.2×10^6	0.6	0.3
32	"	**33)2PD$^+$**	$1.2(1) \times 10^6$		6.2×10^6	1.9	−0.4[g]
33[g]	"	**FeCp*Cp$^+$**	$1.1(1) \times 10^6$		1.0×10^6	1.1	−0.06
34	**FeCp*$_2$**	**33N)$_2^+$**	$5.9(2) \times 10^5$		5.5×10^5	1.1	−0.0
35[e]	**33N)$_2$**	**21/21+**	$2.09(5) \times 10^3$		2.1×10^3	1.0	0.0
36	**21/u22**	**k33NN33+**	$1.13(5) \times 10^4$		9.5×10^3	1.2	−0.1
37	**21/21**	"	$3.4(1) \times 10^4$		4.0×10^4	0.9	0.1
38	**TMPD**	"	$1.17(6) \times 10^6$		1.1×10^6	1.1	−0.0
39	**FeCp*Cp**	"	$3.5(4) \times 10^5$		3.0×10^5	1.2	−0.1
40	**21/u22**	**k33N)$_2^+$**	$2.2(1) \times 10^5$		1.9×10^5	1.2	−0.1
41	**21/21**	"	$8.3(2) \times 10^5$		7.0×10^5	1.2	−0.1
42	**k33NN33**	"	$3.8(2) \times 10^3$		6.7×10^3	0.6	0.3
43	**FeCp*Cp**	"	$5.3(2) \times 10^6$		5.9×10^6	0.9	0.1
44	**FeCp$_2$**	"	$4.8(2) \times 10^4$		4.8×10^4	1.0	0.0
45	**iPr$_2$N)$_2$**	**cHx$_2$N)$_2^+$**	$1.17(13) \times 10^{-2}$		7.4×10^{-3}	1.6	−0.3
46	**cHx$_2$N)$_2$**	**k33)$_2$PD$^+$**	$1.02(3) \times 10^3$		1.7×10^3	0.6	0.3
47	**k33NN33**	**k33)$_2$PD$^+$**	$4.4(2) \times 10^5$		3.7×10^5	1.2	−0.1

[a] k_{12}(calcd) is calculated using eq 1 and k_{ii}(self) from Table 1, for reactions for which k_{ii}(self) is known for both reactants. [b] k_{12}'(calcd) is calculated using the best fit k_{ii}(fit) values from Table 1. [c] $\Delta G_{ij}^{\ddagger}$(obsd) − $\Delta G_{ij}^{\ddagger}$(calcd) for k_{12}'(calcd). [d] From ref 1. [e] From ref 3. [f] There is an error in the k_{12} reported in ref 3; this is the correct value. [g] From ref 2.

Determination of k_{ii}(self) for iPr$_2$N)$_2^{0/+}$

The small k_{ii} value obtained for **iPr$_2$N)$_2$** in stopped-flow experiments encouraged us to use direct measurement of k_{ii}(self) by mixing deuterium-labeled neutral hydrazine with unlabeled radical cation.[3] We employed material having a single isopropyl group substituted as $CH(CD_3)_2$ (see Experimental Section). The NMR signals of the paramagnetic radical cations do not occur in the region examined, and electron exchange is slow on the NMR time scale. Labeled **iPr$_2$N)$_2$-d$_6$** shows a narrow doublet (J = ca. 1 Hz) in its ^{2}H NMR, which decreases to half its initial intensity after complete equilibration with 1 equiv of neutral, unlabeled material. The ion concentrations of the solutions used in the NMR measurements were 0.05−0.06 M, while the stopped-flow reactions were conducted in 0.1 M tetrabutylammonium perchlorate at far smaller radical ion concentrations. We could not use 0.1 M perchlorate because of the insolubility of the hydrazine radical cation perchlorates, but carried out one run in acetonitrile containing 0.1 M tetrabutylammonium tetrafluoroborate and obtained the same rate constant, supporting the assumption that ion-pairing does not significantly affect k_{ii} measurements in acetonitrile. Although the change in relative intensity is smaller, use of ^{1}H NMR for analysis gives better data because of improved signal-to-noise and smaller acquisition times, which allow the collection of more data points. The rate

(7) The total error in solving the simultaneous equations drops very slightly if Z is lowered and reaches a minimum when all Z values are fixed at 2×10^9. This improves the fit of k_{ii}(fit) to k_{ii}(self) for the hydrazines [principally because **22/22**, which has the lowest $E^{\circ\prime}$ and hence the largest K_{12} values and smallest f_{12} values, has a lower k_{12}(fit) than k_{12}(self)], but makes the fit worse for the ferrocenes. If $Z_{11}Z_{22} = (Z_{11} + Z_{22})^2/4$ is used with Z_{ii} values chosen by compound class, raising Z_{ii} for the ferrocenes from the 2×10^9 M^{-1} s^{-1} which fits the hydrazines best to 2×10^{10} M^{-1} s^{-1} slightly improves the fit, but not significantly. Lowering Z_{ii} for PD-derivatives continuously improves the total fit all the way down to Z_{ii}(PD) $= 2 \times 10^3$ M^{-1} s^{-1} and also raises k_{ii}(fit) toward k_{ii}(self) but hardly affects anything but the PD-derivative numbers, and there is certainly no physical justification for this effect, which we believe only occurs because of the large scatter for the k_{12} values for reactions involving PD-derivatives. We conclude that introducing additional fitting parameters by letting Z_{ii} values vary does not significantly help eq 1 fit better, and we see no justification for doing it.

Table 3. Experimental Rate Constant for the Self-Exchange ET Reaction of **iPr$_2$N)$_2$**

expt	signal used	T (°C)[a]	k_{ii}(self) M^{-1} s^{-1}
1	^{2}H	25.9	0.0034
2	^{2}H	25.9	0.0029
3[b]	^{2}H	25.1	0.0034[b]
4	^{1}H	25.6	0.0031

[a] Spectrometer probe set at 298 K; temperatures listed are independently measured using a methanol thermometer (see Experimental Section). [b] In acetonitrile containing 0.1 M tetrabutylammonium tetrafluoroborate. The other experiments used acetonitrile for ^{2}H and acetonitrile-d_3 for ^{1}H NMR detection.

Table 4. Comparison of Geometries at Nitrogen for Crystal Structures Reported Here

compound	d(NN) (Å)	α_{av}(N) (deg)	twist θ(NN) (deg)[a]
iPr$_2$N)$_2$, major	1.394(4)	115.8(3)	88.8(5)
iPr$_2$N)$_2$, minor	1.399(5)	115.8(5)	85.6(8)
cHx$_2$N)$_2$, at N$_1$	1.389(7)	116.7(5)	−87.1(6)
cHx$_2$N)$_2$, at N$_2$		116.6(5)	−87.9(6)
k33)$_2$PD$^+$	1.361(3)[b]	119.9(2)	1.0(4)[c]
k33N)$_2$	1.504(3)	108.4(2)	180
33N)$_2$[d]	1.505(3)	108.0(1)	180

[a] Calculated from the heavy atom positions, assuming the lone pairs bisect the CNC angles in a projection down the NN bond. [b] N−C$_{Ar}$ distance. [c] Nitrogen lone pair, aryl p orbital twist. [d] Nelsen, S. F.; Hollinsed, W. C.; Kessel, C. R.; Calabrese, J. C. *J. Am. Chem. Soc.* **1978**, *100*, 7876.

constant obtained using ^{1}H NMR is indistinguishable from those using ^{2}H NMR. The k_{ii}(self) values obtained in these experiments are summarized in Table 3.

Crystal Structures

Although we previously reported the X-ray structures of two salts of **iPr$_2$N)$_2$**$^+$,[8] we were unable to obtain a structure of the neutral compound. Due to its globular shape, low molecular weight, and the absence of polar groups on the periphery of the molecule, **iPr$_2$N)$_2$** has a low melting point (42−44 °C) and is quite volatile. Its crystals are very soft and deform at room temperature, and obtaining the crystal structure required all manipulations to be done at −20 °C. Sublimation gives nice-looking, but badly twinned, crystals which did not produce a structure we could solve. **iPr$_2$N)$_2$** is very soluble in several common organic solvents (probably on the order of 1g/mL), but only ca. 15 mg/mL in acetonitrile. Vapor diffusion of acetonitrile into a toluene solution at −25 °C gave crystals which were twinned and disordered, with two conformers present. It was possible to use data from one domain of a twin and to model the disorder. Some constraints had to be put on the disorder, so the accuracy of the bond lengths and angles is not very high; however, it was possible to determine that θ for **iPr$_2$N)$_2$** is near 90° (see Table 4). The nitrogens are equivalent by symmetry, and the parameters for the major and minor conformations are similar. Crystal twinning resulted in an even poorer structure being obtained for **cHx$_2$N)$_2$**. In the monoclinic unit cell obtained ($P2_1/n$), dimensions a and c differ by only 1.3%, preventing formation of a single crystal. There is no symmetry element relating the two nitrogens, and therefore their parameters are different (Table 4). In summary, θ is close to 90° for both neutral hydrazines and the α_{av}(N) values are similar but imprecisely determined. Similar pyramidalities at nitrogen, defined using the average of the bond angles at nitrogen, α_{av}(N), and θ values have been reported[8] for **33NN(iPr)$_2$** and its 3-keto analogue.

(8) Nelsen, S. F.; Chen, L. J.; Powell, D. R.; Neugebauer, F. A. *J. Am. Chem. Soc.* **1995**, *117*, 11434.

Although the neutral species have similar geometries, optical spectra of the radical cations reveal a significant difference between **iPr$_2$N)$_2$**$^+$ and **cHx$_2$N)$_2$**$^+$ in solution. Crystalline **iPr$_2$N)$_2$**$^+$ TsO$^-$·CH$_3$CN is only twisted 8° about its NN bond.[8] Its UV spectrum has a single broad maximum at 282 nm (ϵ = 3200 M^{-1} s^{-1}) in acetonitrile, assigned as the $\pi \rightarrow \pi^*$ transition.[9] **cHx$_2$N)$_2$**$^+$ shows maxima at 276 (ϵ = 2400) nm and 386 (ϵ = 1900) nm, suggesting that two forms are present, one with a nearly untwisted NN bond and another having significantly greater NN twist, presumably because of different nonbonded interactions between the cyclohexyl groups. Twisting at the NN bond is known to increase λ_{max} by decreasing the π,π^* energy gap, both from calculations and the increase observed in λ_{max} as methyl groups are replaced by bulky *tert*-butyl groups: **Me$_2$NNMe$_2$**$^+$, λ_{max} = 303 nm; **tBuMeNNMe$_2$**$^+$, λ_{max} = 331 nm; **tBuMeN)$_2$**$^+$, λ_{max} = 414 nm.[9] Distinctly different **cHx$_2$N)$_2$**$^+$ crystals are obtained with different counterions. The tetrakis[*m*,*m*′-bis(trifluoromethyl)phenyl]boron salt gives colorless crystals which X-ray crystallography shows are nearly or completely untwisted about the NN bond and have the cyclohexyl groups in the same io,io N−C rotamer as that found for **iPr$_2$N)$_2$**$^+$ (see Chart 1 of ref. 8 for illustrations of the N−C rotamers possible). The SbF_6^- salt gives red crystals which are clearly strongly twisted (θ ca. 45°) and not in the N−C io,io rotamer but in approximately C_2 rotomers (possibly ii,oo; all C_2 rotamers are calculated to be significantly twisted). Dissolving the colorless crystals produces reddish solutions immediately, as expected because N−C rotation is rapid on the laboratory time scale (a barrier of 11 kcal/mol has been determined for **iPr$_2$N)$_2$**$^+$).[8] The crystal structures will be reported separately following analysis; we have not yet found proper disorder models for these complex crystals.

The crystal structure of **k33)$_2$PD**$^+$**PF$_6$**$^-$ establishes that the nitrogens are planar and that the nitrogen lone pairs are lined up with the aromatic ring p orbitals (see Table 4); therefore, the cation is a close structural analogue of **TMPD**$^+$, but has considerably enlarged alkyl groups. The carbonyl groups are *anti*. The crystal structure of **k33N)$_2$** also has the carbonyl groups *anti*, θ = 180° by symmetry in the crystal (as does **33N)$_2$**), and d(NN) and α_{av} within experimental error of those for **33N)$_2$** (see Table 4).

Discussion: Applicability of Equation 1 to the Reactions Studied

It has puzzled us that the classical Marcus theory (eq 1), correlates our k_{12}(obsd) values so well, because it employs a constant preexponential factor, ignores tunneling effects, and assumes that only the total vertical free energy barrier λ and exoergicity determine the ET rate constant. The more modern vibronic coupling theory has four fundamental parameters determining the rate constant: a classical vertical barrier component λ_s, a quantum-mechanically-treated component λ_v, an energy for the average frequency coupled to the electron transfer $h\nu_v$, and the electronic coupling matrix element V. The compounds studied clearly have a large range for λ_v (argued to be vanishingly small for ferrocenes and unusually large for hydrazines) and $h\nu_v$ (usually assumed to be ≤300 cm^{-1} for ferrocenes but as high as 1668 cm^{-1} for **TMPD**),[10] making it seem unlikely that eq 1 would predict k_{12} quantitatively for cross reactions among them. Nevertheless, eq 1 works well. We have therefore carried out model vibronic coupling theory calculations

(9) Nelsen, S. F.; Blackstock, S. C.; Yumibe, N. P.; Frigo, T. B.; Carpenter, J. E.; Weinhold, F. *J. Am. Chem. Soc.* **1985**, *107*, 143.

(10) (a) Grampp, G.; Jaenicke, W. *Ber. Bunsen-Ges. Phys. Chem.* **1984**, *88*, 325. (b) Grampp, G.; Jaenicke, W. *Ibid.* **1984**, *88*, 335. (c) Grampp, G.; Jaenicke, W. *Ibid.* **1991**, *95*, 904.

Table 5. Model Parameters for ET Used in Calculations

type[a]	V^b	$\lambda_s{}^b$	$\lambda_v{}^b$	λ^b	$h\nu_v{}^c$	$k_{ii}{}^d$
HY	0.1	10	40	50	800	8.86×10^3
FE	0.1	10	15	25	300	1.12×10^7
PD	0.1	10	10	20	1500	7.66×10^8

[a] Parameters mimicking: HY = hydrazine, FE = ferrocene, PD = *p*-phenylenediamine. [b] Unit: kcal/mol. [c] Unit: cm^{-1}. [d] Unit M^{-1} s^{-1}, assuming $K_{eq} = 1$ for preassociation.

using Jortner's double-sum Franck−Condon factor (eq 2),[11] which is applicable to reactions of any size of V, where $S = \lambda_v/h\nu_v$, to see what behavior would be expected using more modern theory. We inserted $K_{eq} = 1\ M^{-1}$ for precursor complex

$$k_{12}(\text{Jor}) = K_{eq}[4\pi^2/h]V^2FC_{v,w}(\text{g}) \qquad (2a)$$

$$FC_{v,w}(\text{g}) = (4\pi\lambda_s k_B T)^{-1/2}[\textstyle\sum_v \exp(-vh\nu_v/RT)]^{-1} \sum_v \sum_w F(v,w) \times \exp(-vh\nu_v/RT)\exp[-(\lambda_s + \{w - v\}h\nu_v + \Delta G^\circ)^2/4\lambda_s RT] \qquad (2b)$$

$$F(\text{v,w}) = \exp(-S)v!w![\textstyle\sum_r\{(-1)^{v+w-r}S^{(v+w-r)/2}\}/\{r!(v-r)! \times (w-r)!\}]^2 \qquad (2c)$$

formation into the expression for k_{12}(Jor) to get the units correct for intermolecular ET reactions. Values for K_{eq} above 0.3 M^{-1} have been argued to be correct for **TMPD**$^{0/+}$.[10,12] To simplify our considerations, λ_s was fixed at 10 kcal/mol, which is close to the experimental value obtained from solvent effects on k_{ii}(self) for bis-*N*,*N*′-bicyclic hydrazines.[13] We chose model parameter sets HY, FE, and PD (HY representing hydrazine, FE ferrocene, and PD phenylenedimine parameters), assigning $h\nu_v$ values of 800, 300, and 1500 cm^{-1}, respectively, and choosing λ_v values to make k_{ii}(Jor), the k_{12}(Jor) value at $\Delta G^\circ = 0$, have values of ca. 9×10^3, 1×10^7, and 8×10^8 M^{-1} s^{-1}, respectively, in rough agreement with the experimental k_{ii} values for these three classes of compounds (see Table 5). We first consider what happens when the driving force increases for two compounds having the other ET parameters the same. Figure 1 shows a graphical comparison of the changes in k_{12}(calcd) from eq 1 ($Z_{11} = Z_{22} = 10^{11}$), in behavior using $k_{ii} = k_{ii}$(Jor) at $\Delta G^\circ = 0$, and in k_{12}(Jor) as exoergicity increases for these models for four V values ranging from 0.02 kcal/mol (in the clearly non-adiabatic region) to 1.0 kcal/mol (in the nearly adiabatic region). Also shown for the HY,HY$^+$ model reaction is a dotted line with a slope of $-1/2$, which is the behavior expected if $f_{12} = 1$ in eq 1. We note that use of the traditional $Z_{11} = Z_{22} = 10^{11}$ value causes the adiabatic prediction of eq 1 to lie slightly below the $V \geq 0.1$ kcal/mol curves for the HY,HY$^+$ model set and slightly above such curves for the FE,FE$^+$ model set and to track the PD,PD$^+$ models set closely for the $V = 0.1$ kcal/mol curve. The differences using the two approaches are too small to be detected in our experimental data when V is ≥ 0.1 kcal/mol, except for the PD model when ΔG° becomes <-8 kcal/mol and V is >0.1 kcal/mol (where k_{12} is too large to be experimentally measured anyway). The calculated $V = 0.02$ kcal/mol differences are larger as ΔG° becomes strongly negative for PD,PD$^+$, suggesting to us that the reactions studied here are unlikely to be this strongly nonadiabatic since we do not see the predicted effect of k_{12}(obsd) deviating more from eq 1 behavior as ΔG° becomes more negative. Because λ_v for the PD,PD$^+$ model almost completely disappears at $\lambda_s = 8$ kcal/mol and $V = 0.02$ kcal/mol, we were forced to use this λ_s value. Note that when these parameters, PD,PD$^+$ ET is in the inverted region when $\Delta G^\circ < -6$ kcal/mol, where k_{12}(Jor) starts to decrease with increasing exoergicity. Most of our experimental data are for compounds with very different ET parameters (λ_v and $h\nu_v$). We believe it is clear that the λ values should be averaged, thus $\lambda_{v12} = (\lambda_{v1} + \lambda_{v2})/2$ (and $\lambda_{12} = (\lambda_1 + \lambda_2)/2$). The most reasonable method of averaging for the $h\nu_v$ values is to use the root of the weighted squares sum for the two compounds (eq 3), which is how the averaging is carried out to calculate the average $h\nu_v$ mode from the contributions of all of the modes of a single compound.[5]

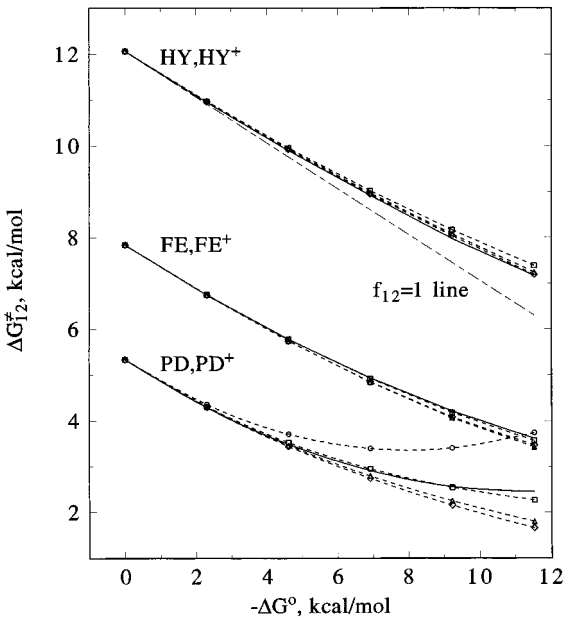

Figure 1. Comparison of calculated effects of exoergicity upon $\Delta G^\ddagger$ for ET for the HY,HY$^+$, FE,FE$^+$, and PD,PD$^+$ model parameters. Solid line: Marcus (eq 1, $Z_{11} = Z_{22} = 10^{11}$ M^{-1} s^{-1}) prediction. Broken lines: Jortner (eq 2) prediction. Squares: $V = 0.1$ kcal/mol. Triangles: $V = 0.5$ kcal/mol. Diamonds: $V = 1.0$ kcal/mol. Circles: $V = 0.02$ kcal/mol, shown only for PD,PD$^+$.

$$h\nu_{v12} = [\{(\lambda_{v1})/(\lambda_{v1}+\lambda_{v2})\}(h\nu_{v1})^2 + \{(\lambda_{v2})/(\lambda_{v1}+\lambda_{v2})\}(h\nu_{v2})^2]^{1/2} \qquad (3)$$

As shown in Table 6, both for calculated HY,FE$^+$ and HY,PD$^+$ reactions, even better agreement between k_{12}′(calcd) and k_{12}(Jor) is obtained. The maximum difference between the two calculations is about 25% out to $\Delta G^\circ = -11.5$ kcal/mol, which corresponds to $\Delta\Delta G^\ddagger$ estimates using eqs 1 and eq 2 being under 0.2 kcal/mol. Surprisingly to us, the effects of large differences in tunneling efficiency are not calculated to detectably affect k_{12}; just knowing k_{ii} values and ΔG° appears to be sufficient to determine k_{12} reasonably well even in the modestly nonadiabatic region. We believe that these calculations rationalize the observed rate data and demonstrate that, despite the assumptions made in its derivation, eq 1 is indeed expected to be adequate for extracting k_{ii} values from experimental data, even when the λ_v and $h\nu_v$ parameters for reaction partners differ greatly and when the reactions are not strongly adiabatic.

Discussion: k_{ii}(fit) Values

All of the k_{ii}(fit) values derived from the cross reaction rate constants (k_{12}(obsd)), are smaller than the independently deter-

(11) (a) Ulstrup, J.; Jortner, J. *J. Chem. Phys.* **1975**, *63*, 4358. (b) Jortner, J.; Bixon, M. *J. Chem. Phys.* **1988**, *88*, 167. (c) Cortes, J.; Heitele, H.; Jortner, J. *J. Phys. Chem.* **1994**, *98*, 2527.

(12) The size of K_{eq} for electron transfer reactions in general remains unknown. Since we are interested here in the effect of driving force on k_{12}, any value could be chosen. If K_{eq} varied widely in real reactions, eq 1, which does not consider it, would work less well.

(13) Table 1, footnote *f*.

Table 6. Comparison of Marcus and Jortner Calculated k_{12} (K_{eq} for preassociation = 1) as a Function of Driving Force for Reactions Where the Components Have Different ET Parameters

$\Delta G°$	Marcus k_{12}	Jortner k_{12}	Jortner/Marcus ratio	$\Delta\Delta G^{‡}$
		HY,FE^{+a}		
0	3.15×10^5	3.52×10^5	1.12	−0.07
−2.31	2.05×10^6	2.22×10^6	1.08	−0.05
−4.61	1.14×10^7	1.18×10^7	1.03	−0.02
−6.92	5.51×10^7	5.39×10^7	0.98	+0.01
−9.22	2.29×10^8	2.10×10^8	0.92	+0.05
−11.53	8.17×10^8	7.07×10^8	0.86	+0.09
		HY,PD^{+b}		
0	2.60×10^6	3.33×10^6	1.24	−0.13
−2.31	1.67×10^7	1.97×10^7	1.18	−0.10
−4.61	8.92×10^7	9.65×10^7	1.08	−0.05
−6.92	3.99×10^8	3.83×10^8	0.96	+0.02
−9.22	1.49×10^9	1.26×10^9	0.85	+0.10
−11.53	4.65×10^9	3.51×10^9	0.75	+0.17

[a] Using $\lambda_{s12} = 10$, $\lambda_{v12} = 27.5$, $V = 0.1$ kcal/mol, $h\nu_{v12} = 700$ cm^{-1}. [b] Using $\lambda_{s12} = 10$, $\lambda_{v12} = 25$, $V = 0.1$ kcal/mol, $h\nu_{v12} = 981$ cm^{-1}.

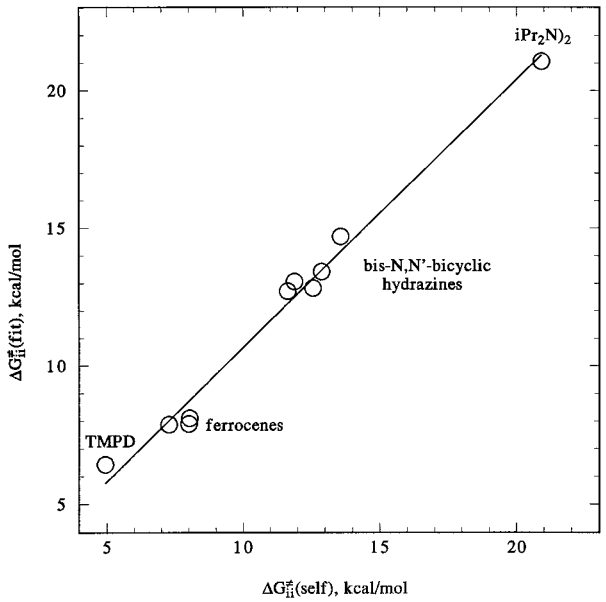

Figure 2. Correlation between $\Delta G_{ii}^{‡}$(fit) and $\Delta G_{ii}^{‡}$(self) from Table 1.

mined homogeneous k_{ii}(self) values except for **FeCp*Cp**$^{0/+}$, where the k_{ii}(self)/k_{ii}(fit) ratio is 0.85. Similar deviations are observed for transition metal coordination compound examples (ref. 5b, p 468), so there appears to be a detectable contribution to k_{12} which is not accounted for properly by eq 1. It is more meaningful to examine activation free energy differences because they are linearly related and may be directly compared. Figure 2 shows a plot of $\Delta G_{ii}^{‡}$(fit) vs $\Delta G_{ii}^{‡}$(self). The regression line shown corresponds to $\Delta G_{ii}^{‡}(\text{fit}) = 0.974\Delta G_{ii}^{‡}(\text{self}) + 0.93$, and the average deviation of $\Delta G_{ii}^{‡}$(fit) from this line is 0.45 kcal/mol. The differences [$\Delta G_{ii}^{‡}$(self) − $\Delta G_{ii}^{‡}$(fit)] are shown in the last column of Table 1; the average difference is 0.66 kcal/mol. These two ways of summarizing the data illustrate the small, systematic nature of the deviations of experiment and theory. Four different kinds of experiments were used to obtain the k_{ii}(self) values in Table 1, which span a factor of 4.9×10^{11}. The cross rate studies use the same kind of experiment to cover the entire range, since k_{12} is sensitive to $\Delta G°$, and the accuracy of the $\Delta G°$ measurements from electrochemistry does not significantly depend upon its size. The k_{ii}(fit) values obtained by simultaneously fitting all cross reaction data to eq 1 are very effective at predicting k_{12}(obsd) and are reasonably close to, but somewhat lower than, k_{ii}(self) values.

The k_{ii}(fit) value for **cHx$_2$N)$_2$** is ca. 10 times that for **iPr$_2$N)$_2$** ($\Delta\Delta G_{ii}^{‡} = -1.3$ kcal/mol). One factor predicted to make k_{ii} larger for **cHx$_2$N)$_2$** than for **iPr$_2$N)$_2$** is a smaller λ_s. Using the touching spheres approximation for modeling, the transition state in Marcus's dielectric continuum formula for estimation of λ_s[5] (eq 4) predicts a smaller λ_s for the larger compound **cHx$_2$N)$_2$**.

$$\lambda_s(\text{kcal/mol}) = 332.1\,(2r_{av})^{-1}\gamma \qquad (4)$$

Use of the molecular volumes occupied in the crystal for **iPr$_2$N)$_2$** and **cHx$_2$N)$_2$** 342.56 and 558.15 Å^3, respectively, yields r_{av} of 4.34 and 5.11 Å from the relationship $V = (4/3)\pi(r_{av})^3$, an expected additional contribution of 0.76 kcal/mol to $\Delta G_{ii}^{‡}$ for **iPr$_2$N)$_2$**, or an increase in k_{ii} of **cHx$_2$N)$_2$** by a factor of 3.6. This estimated difference in λ_s accounts for about half of the difference obtained from the cross rate studies, suggesting that some factor in addition to a difference in λ_s is lowering $\Delta G^{‡}$ for **cHx$_2$N)$_2$** relative to **iPr$_2$N)$_2$**. The X-ray crystal structures show that both neutral hydrazines are in θ near 90° conformations. The presence of a more twisted solution conformation for **cHx$_2$N)$_2$**$^+$ than for **iPr$_2$N)$_2$**$^+$ from comparison of their optical spectra suggests that the larger k_{ii} for the former compound may well result from a smaller λ_v value, because λ_v is expected to decrease as the difference in twist between the neutral and cation oxidation states decreases.

We shall consider 9,9′-bis-9-azabicyclo[3.3.1]nonane (**33N)$_2$**) and its derivatives next. We succeeded in measuring k_{ii}(self) in methylene chloride at $8.7(5) \times 10^3$ M^{-1} s^{-1},[2] but were unable to measure it in acetonitrile due to low solubility. The $k_{ii}(CD_2Cl_2)/k_{ii}(CD_3CN)$ ratios were about 5 for **22/u22$^{0/+}$** and **21/u22$^{0/+}$**, allowing us to estimate k_{ii}(self,CD_3CN) for **33N)$_2$** to be 2.2×10^3 M^{-1} s^{-1},[2] which produces k_{ii}(self)/k_{ii}(fit) = 3.2 ($\Delta\Delta G_{ii}^{‡} = -0.68$ kcal/mol), comparable in agreement to those for directly measured compounds. **33N)$_2$** has a 180° lone pair/lone pair twist angle (θ) in both neutral and radical cation oxidation states and, probably as a direct result, exhibits much faster ET than its $\theta \approx 90°$ analogue, **iPr$_2$N)$_2$**. The X-ray average radius of **33N)$_2$**, at 4.371 Å, is only 0.7% larger than that of **iPr$_2$N)$_2$**, so λ_s differences ought to be small. The smaller geometry change for **33N)$_2$** should result in a smaller λ_v value, and the difference in $\Delta G^{‡}$ values of 7.4$_3$ kcal/mol would require a difference in λ_v of 29.7 kcal/mol if only λ_v differed. The nitrogens of **iPr$_2$N)$_2$** are significantly less pyramidal than those of **33N)$_2$**, which would tend to lower λ_v for **iPr$_2$N)$_2$** relative to that for **33N)$_2$**; the θ difference is clearly more important.

The mono- and bis-γ-keto compounds **k33NN33** and **k33N)$_2$** have geometries at their nitrogens and molecular volumes very similar to those of **33N)$_2$**, and we fully expected that all three would have similar k_{ii} values and that the only effect upon k_{12} values using them would be their significant difference in redox potentials, corresponding to a 10.1 kcal/mol more exoergic reaction for oxidation of the same compound by **k33N)$_2$**$^+$ than by **33N)$_2$**$^+$. As shown in Table 1, however, bis-γ-keto substitution lowers k_{ii}(fit) by a factor of 17, corresponding to an increase in $\Delta G_{ii}^{‡}$ of 1.7 kcal/mol. It appears to us that the change in k_{ii} is unlikely to be caused by changes in λ_v, λ_s, or $h\nu_v$ for these very similar compounds. We suggest that the most likely origins for the rate decrease upon replacement of CH_2 by C═O γ to nitrogen are a decrease in V or in equilibrium constant for precursor complex formation. It seems reasonable to us that the "hole" would avoid the electron-withdrawing carbonyl group, which might lower V by reducing the fraction of relative orientations which have better electronic overlap.

Replacing the dimethylamino groups of **TMPD** by 9-azabicyclo[3.3.1]nonyl groups in **33)$_2$PD** appears to have little effect on k_{ii}: k_{ii}(fit,**33)$_2$PD**)/k_{ii}(fit,**TMPD**) = 1.46. Even the order of reactivity is in doubt, since obtaining a rate ratio greater

than 1 depends entirely on having entry 32, **33N)$_2$,33)$_2$PD**$^+$, in the data set. Elimination of this reaction (i.e., optimization of the remaining 46 reactions) drops the ratio to 0.68.[14] The important point is that **33)$_2$PD** and **TMPD** have nearly the same k_{ii} value. This is surprising in terms of literature discussion of the probable transition state for **TMPD** self-ET.[10,15] Methylated PD$^+$ salts crystallize with the aromatic rings in parallel stacks having ring interplanar distances in the range of 3.1−3.7 Å.[16] The stacks are strongly tilted for **TMPD**$^+$, placing the C_{Ar}-N atom of one unit roughly above the N atom on the adjacent unit, and Grampp and Jaenicke used 5.46 Å ring centers distance with parallel ring planes in modeling the **TMPD**$^{0/+}$ transition state.[10a,c] Rauhut and Clark[15] found the ring centers distance to be an exceptionally "soft" parameter in calculations of the energy of both PD encounter complexes and transition states for self-ET, noting that the energy increases <0.5 kcal/mol for D_2 symmetry parent [PD,PD]$^+$ ET transition states between 3.55 and 4.95 Å when the rings are parallel. They also noted that calculated V decreases sharply as the ring planes move apart. Thus, it has been considered that the transition states for ET which will lead to rapid ET in PD-derivatives are those which have the rings parallel and the π systems overlapping, as they do in crystals, to maximize V. We think it is significant that **33)$_2$PD** has about as large a k_{ii} as **TMPD**, because its large alkyl groups preclude significant aryl ring overlap. Crystalline **33)$_2$PD**$^+$**PF$_6$**$^-$ has the ring stacks slightly less tilted than **TMPD**$^+$, with an interplanar distance of 4.88 Å, 1.33 and 1.50 Å larger than for **TMPD**$^+$**ClO$_4$**$^-$ and -**Br**$^-$ respectively,[16b] and a 6.69 Å ring centers distance. The only way that π-aryl-overlapped transition states could be attained for **33)$_2$PD** would be to fix the *N*,*N* axes perpendicular to avoid nonbonded interaction. Restricting the ET to such a small subset of approaches would be expected to cost entropy relative to **TMPD**, where there is no such requirement, which would be expected to lower k_{ii}. The large k_{ii}(fit) for **33)$_2$PD** indicates that the π-overlapping "stacked" transition state for **TMPD** is not as important a factor in determining k_{ii} as has been believed.

Bis-γ-keto substitution in going from **33)$_2$PD** to **k33)$_2$PD** lowers k_{ii}(fit) by a factor of 4.4 with the 47 reaction data set (2.2 with the 46 reaction data set). This effect is significantly smaller than for the **33N)$_2$** hydrazines, which lack the *p*-phenylene bridging group between the nitrogens, and seems qualitatively consistent with the lowered V for regions near the keto groups mentioned above, since regions near the keto groups would block a smaller fraction of the molecule, but we do not know how to quantitate such an idea.

The preexponential term of ET rate constants using vibronic coupling theory contains V^2 (see eq 2a); therefore, using eq 1 involves an implicit assumption that $V_{12} = (V_{11}V_{22})^{1/2}$. With the wide range of structures used, we expect V_{ii} to vary significantly; however, eq 1 correlates with k_{12}(obsd) well, so the assumption that $V_{12} = (V_{11}V_{22})^{1/2}$ is apparently a rather good approximation. The consistently slightly smaller k_{ii}(fit) than k_{ii}(self) values might, however, be caused by somewhat different V values for the two types of experiments. We expect V to be affected both by orbital overlap and relative orbital energies and to be a maximum when the orbital energies are the same. Changes in overlap may be accounted for well by the averaging used, but cross reactions will have different orbital energies, which we expect to tend to make V_{12} smaller than $(V_{11}V_{22})^{1/2}$. This would be expected to make the k_{ii}(fit) values smaller than the k_{ii}(self) values as observed, because the self-exchange reactions would not suffer from the orbital energy mismatch effect, and might be expected to have larger V values. We note that the largest deviation of k_{ii}(fit) from k_{ii}(self) occurs for **TMPD**, an unhindered aromatic system which might be able to achieve a larger V_{ii} in its self-exchange reaction than in reactions with any of the hydrazines or ferrocenes used in this work.

Discussion: Comparison with Transition Metal Complex Cross Rate Studies

Wherland has reviewed outersphere ET reactions of metal complexes in nonaqueous solvents.[17] Macartney and co-workers have studied many cross reactions of metal-centered systems with +2/+3 charges in acetonitrile, where work terms are presumably important, and all reactions were analyzed using the form of eq 1 containing work terms.[18] For Co(bpyO$_2$)$_3^{2+/3+}$ reactions with ten ML$_3^{3+/2+}$ (M = Fe and Os, L = 2,2′-bipyridyl and 9,10-phenanthroline derivatives), cross rate theory gave k_{ii}(Co) values in the range of 0.8−2 M^{-1} s^{-1},[18a] while for Mn(urea)$_6^{3+/2+}$ reactions with 17 ML$_3^{2+/3+}$ (M = Fe, Os, and Ru), k_{ii}(Mn) varied by over a factor of 1400, from 6.2 × 10^{-3} to 4.4 × 10^{-6} M^{-1} s^{-1}.[18b] Futhermore, both the Co and Mn complexes produce far larger k_{ii} values when Ni(macrocyclic ligand)$^{3+/2+}$ components are employed, k_{ii}(Co) values of 50−600, and k_{ii}(Mn) values of 0.14−0.19 (using k_{ii}(Ni) values, which are range from 1 to 6 × 10^3 M^{-1} s^{-1}, obtained using cross rate theory with other complexes).[18c] These reactions do not follow cross rate theory very quantitatively at all, but how important the work term corrections are in causing this result remains unclear to us. Wherland and co-workers have studied 14 cross reactions between 0 and +1 states of cobalt clathrochelates with ferrocene derivatives[19a] and other cobalt clathrochelates[19b] in acetonitrile. These reactions, which do not involve work term corrections, follow eq 1 with great precision.[19c]

Summary and Conclusions

Equation 1 predicts k_{12} values with remarkable consistency, with few discernable trends over a wide range of $\Delta G°$, $\Delta G_{ii}^{\ddagger}$, and reactant structures. Cross reaction data allow estimates of k_{ii} < 5 × 10^2 M^{-1} s^{-1}, where k_{ii}(self) cannot be determined (without labeling experiments, which require extremely small values) because of insensitivity of both the ESR and NMR spectra to electron exchange when it is so slow. Three principal points of interest in the k_{ii}(fit) values obtained were found: (a)

(14) That there is a problem is most easily seen by examining reaction pairs having a common third component. Dividing the k_{12}(obsd) values for such cases allows direct calculation of the k_{ii} ratio for the other components. When this is done for **33)$_2$PD** and **TMPD** oxidation by **iPr$_2$N)$_2$**$^+$ and **cHx$_2$)$_2$**$^+$, the ratios are 0.50 and 0.51, but for the cation reduction by **33N)$_2$**, the ratio is 14!. Deleting reaction 32 increases $\Delta G_{ii}^{\ddagger}$ for **33N)$_2^{0/+}$** by 0.14 kcal/mol and for **33)$_2$PD$^{0/+}$** by 0.45 kcal/mol, while all the other values change by ≤0.05 kcal/mol. Deleting reaction 32 changes the relative rate constants for **33N)$_2^{0/+}$/k33NN33$^{0/+}$/k33N$_2^{0/+}$** from 17.2:5.6:1 to 14.1:5.6:1.

(15) Rauhut, M.; Clark, T. *J. Am. Chem. Soc.* **1993**, *115*, 9127.

(16) (a) Tanaka, J.; Mizuno, M. *Bull. Chem. Soc. Jpn.* **1969**, *42*, 1841. (b) de Boer, J. L.; Vos, A. *Acta Crystallogr.* **1972**, *B28*, 835.

(17) Wherland, S. *Coord. Chem. Rev.* **1993**, *123*, 169−99.

(18) (a) Macartney, D. H.; Mak, S. *Can. J. Chem.* **1992**, *70*, 39. (b) Macartney, D. H. *Inorg. Chim. Acta* **1987**, *127*, 9. (c) Aquino, M. S.; Foucher, D. A.; Macartney, D. H. *Inorg. Chem.* **1989**, *28*, 3357.

(19) (a) Borchardt, D.; Wherland, S. *Inorg. Chem.* **1986**, *25*, 901. (b) Gribble, J.; Wherland, S. *Inorg. Chem.* **1989**, *28*, 2859. (c) When the least squares fitting procedure is used, $|\Delta\Delta G_{ij}^{\ddagger}|$ averages to 0.05 kcal/mol. The k_{ii}(fit), M^{-1} s^{-1} values obtained are **FeCp$_2$** = 9.18 × 10^6 and **FeCp′$_2$** = 6.74 × 10^6, and the values for five of the clathrochelates are similar to those reported using input k_{ii} values for the ferrocenes.[19a] However, examining this data set illustrates an important point about using the least squares fitting procedure. The data set contains 10 components and 14 reactions, so few components appear in more than three cross reactions. Because the two (BBu)$_2$-containing examples were only reacted with **FeCp*$_2$** and only one of all three of these components was run versus a different component, this subset of reactions is underdetermined and the least squares program cannot correctly determine the related k_{ii}(fit). For the fitting approach employed here to be effective, it is essential that sufficient data for each component is obtained to allow the independent determination of each k_{ii} being fitted in the data set.

The k_{ii}(fit) are systematically lower than k_{ii}(self) by a small, but significant, amount which we suggest might be caused by a smaller *V* for cross than for self-ET reactions. (b) Hindering the approach of the aromatic rings by replacing the Me2N groups of **TMPD** by 33N groups in **33)$_2$PD** changes $\Delta G_{ii}^{\ddagger}$ very little (0.3 kcal/mol or less); thus, close approach of the π faces of the aromatic rings is not required for fast ET, as had been suggested in the literature. (c) Bis-γ-keto substitution in going from 33N to k33N rings raises $\Delta G_{ii}^{\ddagger}$(fit) by about 1.7 kcal/mol in the hydrazine system 33N)$_2$ and by about 1.0 kcal/mol in the aromatic system **33)$_2$PD**; therefore, despite the fact that the geometry at the nitrogens remains almost unaffected, the change in barrier is more important than substantially increasing the distance between the centers of the molecules in b.

Experimental Section

The preparations of most of the compounds used have been described (see the footnotes to Table 1). Cross reaction rate constant were obtained by analysis of absorbance vs time data obtained using either an Applied Photophysics model SX17MV stopped-flow and data analysis system or a Durrum Model D-110 stopped-flow interfaced with On-Line-Instrument-Systems data aquisition and analysis software. The reaction between **cHx$_2$N)$_2$ and iPr$_2$N)$_2$** was so slow that absorbance vs time data were obtained using a Hewlett-Packard 8452 diode array spectrophotometer following manual mixing of reactants in a thermostated cell. Data analysis for this reaction was done using Applied Photophysics software supplied with the SX17MV spectrometer. Reactant solution preparation and handling have been described.[2]

1,1-Dicyclohexylhydrazine. (*Note: nitrosoamines are carcinogenic and mutagenic.*) A solution of 52.26 g (0.248 mol) of *N*-nitrosodicyclohexylamine in 220 mL dry THF was added over 1 h to a stirring mixture of 16.93 g (0.445 mol) of $LiAlH_4$ in 200 mL of dry THF, and the mixture was refluxed overnight and stirred at room temperature an additional day. The mixture was cooled in a dry ice−acetone bath and worked up by slow addition of 15 mL of H_2O followed by 120 mL of 20% NaOH. The aqueous layer was extracted with 2 × 150 mL of Et_2O, and the combined organic layers were dried with magnesium sulfate and concentrated to give 36.6 g of a colorless oil which was Kugelrohr distilled at 80−85 °C (0.03 Torr) to give 35.51 g (0.181 mol, 73%) of 1,1-dicyclohexylhydrazine: ^{1}H NMR ($CDCl_3$) δ 2.63 (br s, 2H), 2.45 (m, 2H), 1.78−1.6 (m, 10H), 1.25−0.9 (m, 10H); ^{13}C NMR ($CDCl_3$) δ 60.83 (CH), 29.18 (CH_2), 26.20 (CH_2), 25.61 (CH_2). Empirical formula was established by mass spectrometry: calcd for $C_{12}H_{24}N_2$ 196.19395, obsd *m*/*e* 196.1940 (57.9%).

Tricyclohexyhydrazine. A mixture of 1,1-dicyclohexylhydrazine (12.06 g, 62 mmol), cyclohexanone (6.56 g, 67 mmol), 50 mL of acetonitrile, and 0.3 mL of acetic acid was stirred for 30 min and treated with $NaBH_3CN$ (4.20 g, 67 mmol), and an additional 50 mL of acetonitrile was added by syringe, followed by 40 mL of methanol to dissolve the white solid present. The reaction mixture was stirred and refluxed, 0.15 mL of acetic acid was added every 15 min for 3 h, and reflux was continued for 2 h. After the solution was cooled overnight, the mixture was treated with 40 mL of 20% NaOH and extracted with 5 × 100 mL portions of pentane. After the extracts were dried over magnesium sulfate, filtered, and concentrated, the yellow oil obtained crystallized slowly. Recrystallization from methanol gave 6.81 g (24.5 mmol, 40%) of tricyclohexylhydrazine as a white solid: mp 60.5−61 °C; ^{1}H NMR (C_6D_6) δ 2.70 (tt, J = 10.3, 3.4 Hz, 1H), 2.58 (tt, J = 11.5, 3.4 Hz, 2H), 1.93 (br d, J = 12.8, 2H), 1.83−1.70 (m, 10H), 1.57 (br d, J = 12.3, 3H), 1.42 (qd, J = 12.3, 2.5 Hz, 4H), 1.30−1.05 (m, 12 H); ^{13}C NMR (C_6D_6) δ 61.09 (CH), 57.81 (CH), 33.00, 31.35, 27.05, 26.76, 26.68, 24.41. Empirical formula was established by mass spectrometry: calcd for $C_{18}H_{34}N_2$ 278.2722, obsd *m*/*e* 278.2722 (28.0%).

Tricyclohexyldiazenium Hexafluorophosphate. A solution of tricyclohexylhydrazine (1.95 g, 7 mmol) in 15 mL of freshly distilled methylene chloride was added by cannula, over 10 min, to a solution of $NOPF_6$ (2.60 g, 14.8 mmol) in 10 mL of freshly distilled acetonitrile stirring at −35 °C. After an additional 35 min of stirring, 270 mL of ether was added by syringe, and the product was filtered and dried in a stream of nitrogen, giving 2.45 g (5.8 mmol, 83%) of a greenish yellow solid: ^{1}H NMR (CD_3CN) δ 4.95 (m, 2H), 4.50 (m, 1H), 2.2−1.15 (m, ∼30 H).

Tetracyclohexylhydrazine, cHx$_2$N)$_2$ was prepared analogously to **iPr$_2$N)$_2$**.[8] A mixture of 270 mg of CuI, 36 mL of freshly distilled THF, and 2 M cyclohexylmagnesium chloride (7 mL, 14 mmol) was stirred at 0 °C under nitrogen, and tricyclohexyldiazenium hexafluorophosphate (2.45 g, 5.8 mmol) was added in one portion. The mixture was allowed to warm to room temperature and stir overnight, and then treated with ammonium chloride (0.9 g) in water (40 mL) and extracted with 4 × 160 mL portions of pentane. After the organic phase was dried with magnesium sulfate, filtered, and concentrated, the residue was recrystallized from toluene and acetonitrile to give the hydrazine as a white solid, 0.933 g (2.6 mmol, 44%): mp 194−196 °C. ^{1}H NMR (C_6D_6) δ 2.74 (tt, J = 12, 3 Hz, 4H), 1.90 (br d, J = 12 Hz, 8H), 1.78 (br d, J = 13 Hz, 8H), 1.67−1.56 (m, 12H), 1.26 (qt, J = 13, 3.5 Hz, 8H), 1.08 (qt, J = 13, 3.5 Hz, 4H); ^{13}C NMR (C_6D_6) δ 61.99, 34.80, 27.49, 26.68. Empirical formula was established by mass spectrometry: calcd for $C_{24}H_{44}N_2$ 360.3505, obsd *m*/*e* 360.3486 (30.0%). The structure was confirmed by X-ray crystallographic analysis.

Tetracyclohexylhydrazine Radical Cation Hexafluoroantimonate, cHx$_2$N)$_2^+$SbF$_6^-$. $AgSbF_6$ (81.0 mg, 0.236 mmol) was weighed out in a 50 mL Schlenk flask under nitrogen and dissolved in CH_2Cl_2 (3 mL). Tetracyclohexylhydrazine (85.0 mg, 0.236 mmol) was added as a solid resulting in a greenish-black solution. After 5 h of stirring, the mixture was filtered through Celite and the filter was rinsed with CH_2Cl_2 (5 mL). The bright-red solution was evaporated to give a red solid that was dissolved in minimum amount of CH_2Cl_2 (*ca* 3 mL). Precipitation with ether afforded the product (119 mg, 84%). Recrystallization by vapor diffusion of ether into a CH_2Cl_2 solution proceeded very quickly and gave large but rather shapeless crystals, whereas recrystallization by vapor diffusion of ether into acetonitrile solution proceeded much slower, giving small but very well-developed prisms. The structure of the radical cation was confirmed by X-ray crystallographic analysis of a prism from CH_3CN recrystallization.

1,4-Bis(3′-keto-9′-azabicyclo[3.3.1]non-9′-yl)benzenium Hexafluorophosphate, k33)$_2$PD$^+$PF$_6^-$. A solution of $NOPF_6$ (0.59 g, 3.35 mmol) in 10 mL of acetonitrile was added by cannula to the neutral compound (Table 1, footnote *k*, 1.18 g, 3.35 mmol) in 50 mL of CH_2Cl_2, under nitrogen, and the mixture was stirred overnight. The blue residue, after solvent removal, was crystallized by vapor diffusion of ether into acetonitrile, giving 0.55 g (1.3 mmol, 40%) of the salt, which was characterized by obtaining an X-ray crystal structure.

Crystal structure data and refinement parameters for **iPr$_2$N)$_2$**, **cHx$_2$N)$_2$**, **k33)$_2$PD$^+$PF$_6^-$**, and **k33N)$_2$** appear in the Supporting Information.[20]

Acknowledgment. We thank the National Science Foundation for partial financial support of this work under Grants CHE-9504133 (J.R.P.) and −9417946 (S.F.N.). Acknowledgement is also made to the donors of the Petroleum Research Fund, administered by the ACS for partial support of the research under grant ACS-PRF 29982-B4 (JRP). We thank Fred King for assistance with Fortran programming.

Supporting Information Available: Experimental for determination of ET rate constants for **iPr$_2$N)$_2^{0/+}$** by ^{2}H and ^{1}H NMR, and crystal data for **iPr$_2$N)$_2$**, **cHx$_2$N)$_2$**, **k33)$_2$PD$^+$PF$_6^-$**, and **k33N)$_2$** (5 pages). See any current masthead page for ordering and Internet access instructions.

JA970321J

(20) The authors have deposited atomic coordinates for these structures with the Cambridge Crystallographic Data Centre. The coordinates can be obtained, on request, from the Director, Cambridge Crystallographic Centre, 12 Union Road, Cambridge, CB2 1EZ, U.K.